Propagation of waves through a slab near the Anderson transition: a local scaling approach

1990 J. Phys.: Condens. Matter 2 307

(http://iopscience.iop.org/0953-8984/2/2/007)

J. Phys.: Condens. Matter 2 (1990) 307–321. Printed in the UK

Propagation of waves through a slab near the Anderson transition: a local scaling approach

R Berkovits and M Kaveh
Department of Physics, Bar-Ilan University, Ramat-Gan, Israel

Received 30 May 1989

Abstract. We use a local scaling approach to calculate the following properties near the Anderson transition:

(i) the time-dependent pulse shape of the transmitted wave through a slab;
(ii) the wavelength dependence of the intensity–intensity autocorrelation function $C(\Delta\lambda)$;
(iii) the time dependence of the intensity–intensity autocorrelation function $C(\Delta t)$ for dynamic disorder;
(iv) the correlation function for the memory effect.

Our local scaling approach is shown to be consistent with Anderson's global scaling theory and yields the same scaling behaviour for the transmission coefficient. All the correlation functions are shown to depend explicitly on the averaged intensity pulse shape for small values of $\Delta\lambda$ or Δt.

1. Introduction

Propagation of classical waves (optical or acoustical) through random media has recently aroused renewed interest mainly due to the prediction [1, 2] of the possibility of localising these waves. The localisation of a wave is expected to occur when the Ioffe–Regel condition [3] is obeyed, namely, when $Kl = 1$, where $K = 2\pi/\lambda$ is the wave number of the wave, λ the wavelength and l the elastic transport mean free path. Until now the Ioffe–Regel condition was achieved [4–6] only for quantum waves (electrons) and indeed for strong disorder a metal-insulator transition was widely observed [7]. Experimentally [8, 9] it was found that below some critical disorder the electron diffusion constant (extracted from the conductivity) vanishes with a critical exponent $\nu = 1$ or $\nu = 1/2$. This non-universality behaviour is believed [6, 10, 11] to be a consequence of the long-range electron–electron interactions which strongly affect the diffusion constant in the presence of disorder. A pure localisation transition, which is termed an Anderson transition, is extremely difficult to observe due to the effects of electron–electron interactions [12]. Therefore, localisation of classical waves which are free from particle–particle interactions have the potential of serving as a decisive test for the nature of the Anderson transition. The realistic conditions for a particular material to show classical localisation was recently studied intensively [13–18]. The most widely used theoretical treatment of the Anderson transition is the one-parameter scaling theory [19]. Its main predictions are a universal critical exponent $\nu = 1$ and a scale-dependent diffusion

0953-8984/90/020307 + 15 $03.50

constant $D = D_0(l/L)$ (for a three-dimensional system), where L is the length of the system in a cube geometry. Experimentally, both of these predictions are difficult to observe [6, 8, 9] for electron systems. The electron–electron interactions affect both predictions. There are materials which show a critical exponent $\nu = 1/2$ and the length dependence of D as deduced from its *temperature* dependence is also not universal [12]. On the theoretical side, calculations [20, 21] of higher moments of the conductance seem *not* to follow a one-parameter scaling theory. It is therefore hoped that detailed experiments on optical systems may clarify the nature of the Anderson transition. Recent optical experiments [22] report an impressive small free path, almost equal to the Ioffe–Regel limit. In order to enable specific predictions for various optical properties near the Anderson transition, we use the scaling theory to calculate these properties. In particular, we calculate: (i) the time dependence of transmitted pulses; (ii) the wavelength dependence of the static intensity autocorrelation functions; (iii) the time dependence of $C(\Delta t)$ for dynamic disorder, and (iv) the memory effect.

In order to motivate future experiments, we use the slab geometry. We hope that our specific predictions will serve as a guide to probe out the optical Anderson transition and to check the validity of the scaling theory.

2. The scaling theory of the optical Anderson transition

The scaling theory for the electron conductance resulted in a scale-dependent diffusion constant

$$D = \begin{cases} D_0(l/\xi) & L > \xi \\ D_0(l/L) & L < \xi \end{cases} \tag{1}$$

for a *cube* of size L and ξ is the correlation length [23]

$$\xi = l\,|(\lambda - \lambda_c)/\lambda_c|^{-\nu} \tag{2}$$

above the transition and the localisation length below the transition [19]. It is easy to show that for a slab geometry, equations (1) and (2) still hold where L is now the width of the slab.

Using (1), Anderson predicted [2] that the averaged transmission coefficient of a wave near the transition will change from $T = l/L$ in the weak-disorder limit ($l \gg \lambda$) to

$$T = (l/L)^2 \qquad L < \xi \tag{3}$$

in the strong-disorder limit, $l \simeq \lambda$.

John [1] was the first to stress the importance of absorption near the optical Anderson transition. Later, Anderson predicted [2] that in the presence of absorption the transmission coefficient will be given by

$$T = \exp[-L/(\tfrac{2}{3}L_a)] \tag{4}$$

where L_a is the absorption length given by $L_a = (l^2 l_i)^{1/3}$ and l_i is the inelastic mean free path.

The advantage of studying optical (or acoustical) waves is the possibility of measuring local intensities and their sensitivity to external changes, such as the wavelength or the direction of the incident wave. These two properties (among many others) depend on the inference between different Feynman trajectories. Both of these properties were

studied intensively in the weak-disorder limit. The first is the intensity–intensity autocorrelation function [25–28] at a given point as a function of the wavelength change $C(\Delta\lambda)$ and the second property is the memory effect [29].

When the nature of diffusion is changed near the Anderson transition, we expect different behaviour of these properties. We need a scaling theory for *local* properties which cannot be extracted from the global scaling property of the diffusion constant as given by equation (1). In the weak-disorder limit, diffusion theory was very successful in accounting for many of the observed interference phenomena. These include the coherent backscattering for different geometries [30–34], the dynamic autocorrelation function $C(\Delta t)$ [35–40], the static autocorrelation function $C(\Delta\lambda)$ [25–28] the diffuse transmitted pulse shape [41] and the memory effect [29, 42, 43]. These effects were calculated in q space using a diagrammatic approach or in real space using the concept of interference between different Feynman trajectories. Both approaches were found to agree [27, 40, 43].

We use here the real space approach and modify the previous approaches by using anomalous diffusion. The diffusion of a wave packet near the transition for $L < \xi$ is modified to obey

$$\langle X^2 \rangle = \alpha t^{2/3} \tag{5}$$

This is consistent with scaling theory since the time needed to diffuse across the sample is now $t \sim L^3$, which means that $D \sim 1/L$. Thus, for a given separation in space, the length of the Feynman path connecting two points is much larger near the transition. This property must modify the interference phenomena which become more sensitive to phase changes.

We therefore assume that the average intensity of the wave obeys a diffusion equation even near the Anderson transition,

$$D(t)\nabla^2 I(\bar{x}, t) = \partial I(\bar{x}, t)/\partial t \tag{6}$$

where $I(\bar{x}, t)$ is the ensemble averaged intensity at position $\bar{x}$ from the incident boundary at time t. The diffusion constant is now time-dependent and from (5) it follows that [44–46]

$$D(t) = \begin{cases} D_0(\tau/t)^{1/3} & t < \xi^3/lD_0 \\ D_0(l/\xi) & t > \xi^3/lD_0 \end{cases} \tag{7}$$

where τ is the elastic scattering time l/C and $D_0 = \frac{1}{3}Cl$. Equation (7) by itself is *not* sufficient to produce the correct scaling behaviour as given by (3). Moreover, it leads to an unphysical divergence in T. The key point is to specify the boundary conditions self-consistently. In the weak-disorder limit, the solution to the Milne equation is made [47] to coincide with the solution of the diffusion equation if one assumes that the wave exits the slab at a distance a from the surface where a is given by

$$a = 3(1 + \Delta)D_0/C \tag{8}$$

where, for a three-dimensional [48] system, $\Delta = 0.714$. We claim that a must be scale-dependent near the transition. In the weak-disorder limit, the transmission can be extracted from the averaged intensity at $X = L - a$ and this leads to

$$T = a/L \tag{9}$$

Near the transition we replace D_0 in (8) by $D(L)$ as given by (1) and this leads to

$$T = (1 + \Delta)\left(\frac{l}{L}\right)^2 \tag{10}$$

in agreement with Anderson's prediction in (3) which was obtained for $\Delta = 0$.

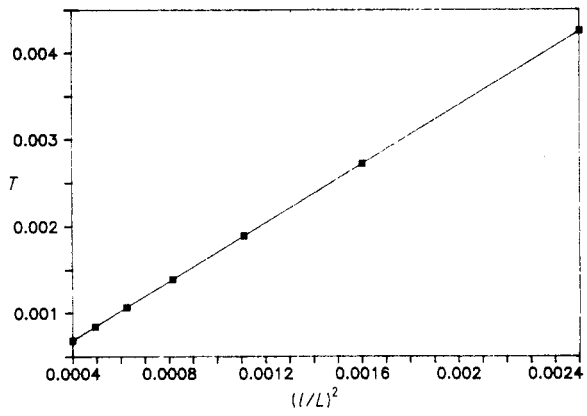

Figure 1. The total transmission, T, for different values of the slab width L. The dots correspond to T calculated by (14) for several values of L. The correlation length was taken to be $\xi = 10^4 l$.

For the properties we calculate in this paper, we need the time-dependent solution of (6). The boundary condition (8) must now be modified to

$$a(t) = 3(1 + \Delta)D(t)/C \tag{11}$$

where $D(t)$ is given by (7). This means that each Feynman path will leave the sample at a *different* plane. If the photon spends more time in the sample, its diffusion constant is reduced and therefore will leave the sample *closer* to the boundary. This idea was introduced [45] to calculate coherent backscattering near the Anderson transition. Here we show that (11) is consistent with Anderson's results as given by (3) and (4). We next use this approach to calculate $C(\Delta\lambda)$ and the memory effect near the Anderson transition.

3. Time-dependent transmission

We now calculate for a slab geometry the time dependence of the transmitted wave for an initial injected narrow pulse. The time dependent transmission is given by $I(x = L - a(t), (t)$. Therefore, we have to calculate $I(x, t)$ which solves the diffusion equation (6) at a distance $a(t)$ from the boundary as given by (11). This leads to

$$T(t) = \frac{2}{L}\sum_{n=1}^{\infty}(-1)^{n+1}\sin^2\left(\frac{n\pi}{L}a\left(\frac{\tau}{t}\right)^{1/3}\right)\exp\left(-\frac{3}{2}D_0\left(\frac{n\pi}{L}\right)^2\tau^{1/3}t^{2/3}\right) \tag{12}$$

for $L < \xi$. Summing up all terms, we get for $t < \tau_1 = \xi^3/Cl^2$

$$T(t) = \left(\frac{1}{2L}\right)\left(\theta_4\left(0\left|\frac{i\pi^2 D_0 T^{1/3}}{L^2}t^{2/3}\right.\right) - \theta_4\left(\frac{\pi a T^{1/3}}{Lt^{1/3}}\left|\frac{i\pi^2 D_0 T^{1/3}}{L^2}t^{2/3}\right.\right)\right) \tag{13}$$

where θ_4 is the theta function.

We now calculate the total transmission T

$$T = \int_0^{\infty} T(t)\,\mathrm{d}t \tag{14}$$

where $T(t)$ is given by (13). In figure 1, we plot T as a function of L and find results consistent with those of Anderson, namely, for $L < \xi$, $T \propto (l/L)^2$.

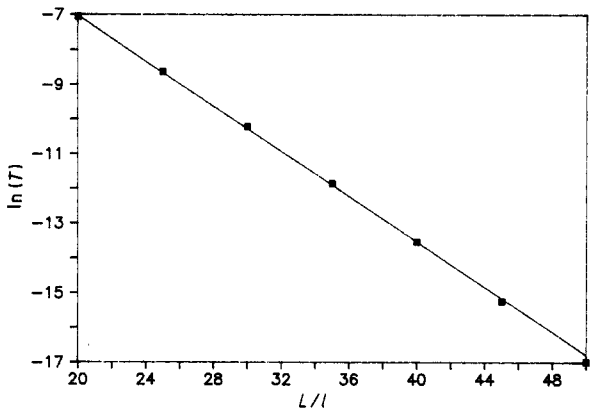

Figure 2. The total transmission for an absorbing slab. The dots correspond to T_{abs} calculated by (16) for several values of L. The absorption length $L_{abs} = 4.64\,l$, the correlation length $\xi = 10^4\,l$. The slope of the line is $-l\ln(T_{abs})/L = 3.02$ which is equal to $2/3L_{abs}$ as predicted in equation (17).

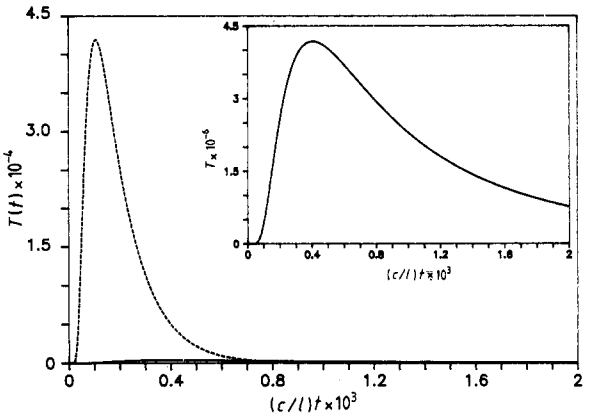

Figure 3. The transmission $T(t)$ as a function of time t. The dashed curve is $T(t)$ for normal diffusion. The full curve is $T(t)$ for anomalous diffusion where the correlation length is $\xi = 10^4\,l$. The inset is $T(t)$ for the anomalous diffusion plotted on a different scale.

We now include absorption effects. Absorption will modify the diffusion (6) by adding a term $-I(\bar{x}, t)\tau_a$ where τ_a is the absorption time. This will modify $T(t)$ in (13) to

$$T_{abs}(t) = \exp(-t/\tau_a)T(t). \tag{15}$$

The total transmission in the presence of absorption is given by

$$T_{abs} = \int_0^\infty T_{abs}(t)\,dt \tag{16}$$

In figure 2, we plot T_{abs} as a function of L and indeed get the Anderson prediction

$$T_{abs} \propto \exp(L/\tfrac{2}{3}L_a) \qquad \xi > L > L_a \tag{17}$$

where $L_a = (l^2 l_i)^{1/3}$. For $L < L_a < \xi$, we get $T \simeq (l/L)^2$.

We therefore stress that the time-dependent transmissions $T(t)$ or $T_{abs}(t)$ are consistent with the scaling hypothesis. This provides a new approach to verifying the scaling theory by measuring the transmitted pulse shape as a function of time. The pulse shape of $T(t)$ as given by (13) is anomalous as is shown in figure 3. Thus, the advantage of using classical waves is that one can measure $T(t)$ directly and not just the total transmission

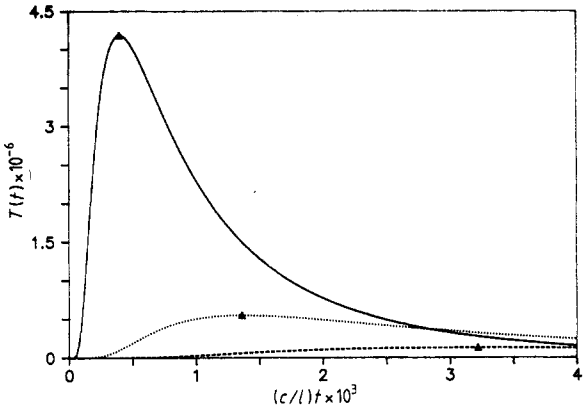

Figure 4. The transmission $T(t)$ for different values of the slabs length L. The correlation length $\xi = 10^4\, l$. The full curve corresponds to $L = 20\, l$. The dotted curve corresponds to $L = 40\, l$ and the dashed curve to $L = 60\, l$. A triangle marker was set on the maximum of each curve to denote t_{max} for each L. t_{max} is proportional to L^3.

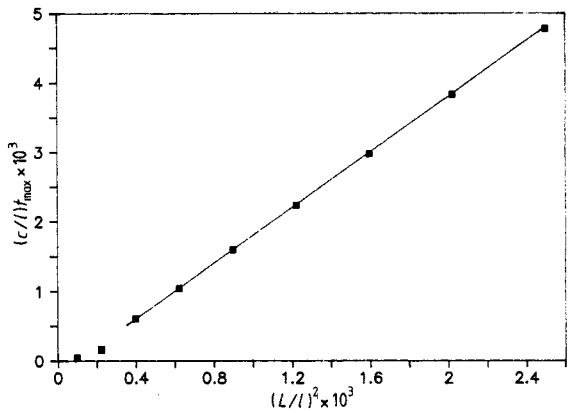

Figure 5. t_{max} for different values of the slab length L. The correlation length $\xi = 5\, l$. For $L \gg \xi$, t_{max} is proportional to L^2. For $L \sim \xi$ there are deviations from that behaviour.

T. To obtain $T(t)$, it is of course not sufficient to know the scale dependence of the diffusion constant (as given by (1)); rather, one needs to know $D(t)$ as given by (7). The asymptotic form of $T(t)$ near the transition is given by

$$T(t\to\infty) \propto (1/t^{2/3}) \exp[-\tfrac{3}{2}D_0(\pi/L)^2\tau^{1/3}t^{2/3}] \tag{18}$$

Note that $T(t)$ falls off *much* slower than in the weak disorder limit, where $T(t\to\infty) \propto \exp[-D_0(\pi/L)^2]$. Moreover, the maximum of $T(t)$ is delayed. It is this delay time which can signal in an experiment the onset of an Anderson transition. The time t_{max} for which $T(t)$ reaches its maximum scales differently with L near the transition. In the diffusive region, $l \gg \lambda$, $t_{max} \simeq L^2/D_0$. In the anomalous diffusion regime for which $l \simeq \lambda$, D_0 must be replaced by $D(L) = D_0(l/L)$ and we therefore expect

$$t_{max} \simeq 3L^3/C\lambda^2 \tag{19}$$

For $L > \xi$, we expect

$$t_{max} \simeq 3L^2\xi/C\lambda^2 \tag{20}$$

In figure 4, we plot $T(t)$ for different values of $L(\xi > L)$.

In figure 5, we plot t_{max} as a function of L as extracted from $T(t)$ which is given by (13). We see a crossover from an L^3 dependence for $L \simeq \xi$. In the case of absorption,

$T_{abs}(t \to \infty) \propto \exp(-t/\tau_a)$ and this asymptotic form is similar to the asymptotic form in the non-anomalous regime. In this case, $T_{abs}(t)$ is not a sensitive probe of anomalous diffusion. Thus, a significant change in the optical properties will be observed only for extremely strong disorder when the localisation length ξ becomes smaller than L_a. This restricts the observability of the Anderson transition to stronger disorder. Thus, absorption is a real obstacle in identifying an Anderson transition. For optical systems, Genack and Drake [22] succeeded in producing a short mean free path $l \simeq \lambda/\pi$ for T_i spheres in air. However, they have found strong absorption effects and concluded that $L_a \simeq \frac{1}{4}L$. In this case, anomalous diffusion is completely suppressed since $L_a < L$. The diffusion constant in this case is also enhanced from $D = D_0(l/L)$ by a factor (L/L_a). Thus, absorption for electro-magnetic waves acts to smear the transition in the same way as finite temperatures for electron systems. The ideal experiment for testing the nature of the Anderson transition must produce a system for which $Kl \simeq 1$ and yet the absorption is small, at least in the sense that the system remains *mesoscopic*, $L_a > L$. For a mesoscopic system, anomalous diffusion is the main characteristic feature of the Anderson transition within the framework of a one-parameter scaling theory.

4. Wavelength dependence of the intensity–intensity autocorrelation function $C(\Delta\lambda)$

The normalised intensity–intensity autocorrelation function $C(\Delta\lambda)$ is given by

$$C(\Delta\lambda) = (\langle I(\lambda)I(\lambda+\Delta\lambda)\rangle - \langle I(\lambda)\rangle\langle I(\lambda+\Delta\lambda)\rangle)/\langle I(\lambda)\rangle^2 \tag{21}$$

$C(\Delta\lambda)$ was studied intensively in the strong disordered limit [49–52] (especially for one dimensional systems) and in the weak-disorder limit [24–28]. In particular, it was demonstrated [27] that the real-space approach, in which $C(\Delta\lambda)$ is a result of interference between different Feynman paths with different phases due to the wavelength change $\Delta\lambda$, leads to results identical to the diagrammatic [25, 26] approach and in excellent agreement with recent experiments [22, 24]. In the real-space approach, $C(\Delta\lambda)$ is given [27] by

$$C(\Delta\lambda) = \left|\sum_N W_N \exp\left(\mathrm{i}\frac{2\pi}{\lambda}\frac{\Delta\lambda}{\lambda}Nl\right)\right|^2. \tag{22}$$

This is obtained within the factorisation approximation [25] in which

$$\langle I(\lambda)I(\lambda+\Delta\lambda)\rangle - \langle I(\lambda)\rangle\langle I(\lambda+\Delta\lambda)\rangle = |\langle E(\lambda)E^*(\lambda+\Delta\lambda)\rangle|^2.$$

In the weak-disorder limit, this approximation was recently checked numerically [28] and was found to be excellent for $C(\Delta\lambda)$ at a given point. This approximation, however, is not valid near the transition due to strong amplitude correlations. Nevertheless, one can still use a heterodyne technique [46] to measure directly the electric field–electric field correlation function $\langle E(\omega)E^*(\omega+\Delta\omega)\rangle$ where ω is the frequency and $\Delta\omega = -(\Delta\lambda/\lambda)\omega$. In the weak-disorder limit, we get from (22)

$$C(\Delta\omega) = |\langle E(\omega)E^*(\omega+\Delta\omega)\rangle|^2 = \left|\int \mathrm{d}t\, \mathrm{e}^{\mathrm{i}\Delta\omega t}T(t)\right|^2 \tag{23}$$

noting that $W_N = T(t)$.

The important question is whether (23) also holds near the transition when $T(t)$ is replaced by the anomalous pulse shape as given by (13). We show that (23) holds *only*

for $\Delta\omega \ll D_0 l/\xi^3$. Generally, we may write for an exit point $x = L - a$, where a is given by (8),

$$E(\omega) = \int e^{-i\omega t} E_\omega(t)\, dt \tag{24}$$

which leads to

$$\langle E(\omega) E^*(\omega + \Delta\omega)\rangle = \int e^{i\Delta\omega t} \langle E_\omega(t) E^*_{\omega+\Delta\omega}(t)\rangle\, dt \tag{25}$$

Near the transition $E_{\omega+\Delta\omega}$ differs significantly from E_ω only for $\Delta\omega > D(L, \xi)/\xi^3$ where $D(L, \xi)$ is given by (1). For $\Delta\omega < D(L, \xi)/\xi^3$, we may approximate $E_{\omega+\Delta\omega}$ by E_ω and (25) then coincides with (23). In this regime, we may obtain the scaling behaviour of $C(\Delta\omega)$ from $T(t)$. For $L < \xi$, the Feynman trajectories smaller than ξ^3/l^2 obey anomalous diffusion. For $t \geqslant L^3/l^2 C$, $T(t)$ scales as $T(t^{1/3}L^{-1})$ which leads to

$$C(\Delta\omega) \sim \left| \int dx\, T(x)\, e^{i\Delta\omega L^3 x} \right|^2$$

which leads to $C(\Delta\omega L^3)$. We have calculated the values of $\Delta\omega$ which correspond to $C(\Delta\omega) = 0.9$ and indeed find that $\Delta\omega \propto 1/L^3$. For $L > \xi$, $C(\Delta\omega)$ scales differently. In this regime most Feynman trajectories obey normal diffusion but with a renormalised diffusion constant $D_0 l/\xi$. For $t \geqslant \xi^3/l^2 C$, $T(t)$ scales as $T(t/L^2\xi)$, which implies that $C(\Delta\omega)$ scales as $C(\Delta\omega L^2 \xi)$. This scaling behaviour of $C(\Delta\omega)$ is valid only for $\Delta\omega < D_0 l/\xi^3$.

As we reach the transition, $\xi \to \infty$ and the interesting region becomes $\Delta\omega > D_0 l/\xi^3$. In this regime (23) is not valid. We calculate $C(\Delta\omega)$ in this regime diagrammatically by using the following ladder propagator

$$L(q, \Delta\omega) = (4\pi C/\Omega l^2)(D(q, \Delta\omega) - i\Delta\omega) \tag{26}$$

where $D(q, \Delta\omega)$ is given by

$$D(q, \Delta\omega) = D_0(\Delta\omega l/C)^{1/3} \qquad q < 1/\xi \text{ and } \Delta\omega > D_0 l/\xi^3 \tag{27}$$

For $\Delta\omega < D_0 l/\xi^3$, $D(q, \Delta\omega)$ is independent of $\Delta\omega$ and is given by

$$D(q, \Delta\omega) = \begin{cases} D_0 lq & q > 1/\xi \\ D_0 l/\xi & q < 1/\xi \end{cases} \tag{28}$$

Thus, $\Delta\omega < D_0 l/\xi^3$, $D(q, \Delta\omega)$ is independent of $\Delta\omega$ and we get exactly the same results as those that follow from (23). For $\Delta\omega > D_0 l/\xi^3$, we know $L(q, \Delta\omega)$ only for $q < 1/\xi$ which yields $C(\Delta\omega)$ for $L > \xi$. Here, unlike in the region where $\Delta\omega \to 0$, $L(q, \Delta\omega)$ is independent on ξ. Using equations (26)–(27), for $L > \xi$ we get for the asymptotic form for $C(\Delta\omega)$

$$C(\Delta\omega) = A(L(\Delta\omega)^{1/3})^{-1} \exp(-BL(\Delta\omega)^{1/3}) \qquad \Delta\omega \gg D_0 l/\xi^3 \tag{29}$$

where $A = (3\sqrt{3}/4l^2)(\pi/\omega\lambda l^2)^{-1/3}$ and $B = (1/\sqrt{2})(3/l^2 C)^{1/3}$. Thus, we see that $C(L, \Delta\omega)$ scales as $C(L(\Delta\omega)^{1/3})$ for $L > \xi$ and $\Delta\omega \gg D_0 l/\xi^3$. This behaviour can be understood as follows. For $\Delta\omega \gg D_0 l/\xi^3$, only short Feynman trajectories are important and contribute to $C(\Delta\omega)$. For short trajectories the slab geometry is not effective in cutting off the trajectories because of the boundaries. Thus, we expect that $C(\Delta\omega)$ will

Table 1. The different scaling results for $C(\Delta\omega)$.

	$\Delta\omega < D_0 l/\xi^3$	$\Delta\omega > D_0 l/\xi^3$
$L < \xi$	$C(\Delta\omega L^3)$	
$L > \xi$	$C(\Delta\omega L^2\xi)$	$C(\Delta\omega^{1/3}L)$

be similar to that obtained for a point source at a distance R from the source when R is replaced by L. For a point source for $\Delta\omega \gg D_0 l/\xi^3$, one can define a dephasing length $L_{\Delta\omega}$

$$L_{\Delta\omega} = (D(\Delta\omega)/\Delta\omega)^{1/2} \tag{30}$$

which is the distance a photon travels in an internal $1/\Delta\omega$. For a point source we know that $C(\Delta\omega) \sim \exp(-R/L_{\Delta\omega})$. We thus claim that in this regime for a slab geometry we must get

$$C(\Delta\omega) \propto \exp(-L/L_{\Delta\omega}) \tag{31}$$

For $\Delta\omega \gg D_0 l/\xi^3$, we must use $D(\Delta\omega)$ from (27) which yields $L_{\Delta\omega} = (Cl^2/\Delta\omega)^{1/3}$. Inserting this $L_{\Delta\omega}$ in (31) leads to the scaling behaviour which we have found diagrammatically and is given by (29).

We summarise in table 1 our scaling results for $C(\Delta\omega)$. For $L > \xi$, we have a crossover from a scaling form $C(\Delta\omega L^2\xi)$ for $\Delta\omega < D_0 l/\xi^3$ to $C(L(\Delta\omega)^{1/3})$ for $\Delta\omega \gg D_0 l/\xi^3$. For $L < \xi$, we know the scaling form for $C(\Delta\omega)$ only for $\Delta\omega < D_0 l/\xi^3$ which behaves as $C(\Delta\omega L^3)$.

We now discuss quantitatively our results. We define $\Delta\omega_0 = D_0 l/\xi^3$ which yields,

$$\Delta\omega_0/\omega_0 = (l/\xi)^3 \tag{32}$$

The half-width frequency $\Delta\omega_{HW}$ is given by

$$\Delta\omega_{HW}/\omega_0 \simeq (l/L)^3 \tag{33}$$

where $\omega_0 = C/l$.

For $L < \xi$, $\Delta\omega_{HW} > \Delta\omega_0$ and we know $C_0(\Delta\omega)$ only for $\Delta\omega \ll \Delta\omega_{HW}$. which means that $C(\Delta\omega) \sim 1$. The form of $C(\Delta\omega)$ for which $C(\Delta\omega) < 1$ is not known by the present approach. For $L > \xi$, $\Delta\omega_{HW} < \Delta\omega_0$ and we know $C(\Delta\omega)$ for the entire range of $\Delta\omega$. In particular, for $L \gg \xi$ and $\Delta\omega_{HW} \ll \Delta\omega_0$, we may obtain $C(\Delta\omega)$ from the anomalous transmitted pulse shape $T(t)$ as given by (23). In figure 6, we plot $C(\Delta\omega)$ as a function of $\Delta\omega/\omega_0$ for $L = 20l$ and $\xi = 10l$. For these values, $\Delta\omega_{HW}/\omega_0 = 10^{-4}$ and $\Delta\omega_C/\omega_0 = 10^{-3}$. From the figure we see that for $\Delta\omega/\omega_0 \sim 10^{-3}$, $C(\Delta\omega)$ dropped almost to zero. Thus, the use of (23) is justified. For comparison, we plot (curve b) $C(\Delta\omega)$ as a function of $\Delta\omega/\omega_0$ by using the normal diffusion shape of $T(t)$ calculated with $D = D_0 = \frac{1}{3}Cl$. We see that $C(\Delta\omega)$ in this case is much broader. This follows from the fact that $C(\Delta\omega)$ is the Fourier transform of $T(t)$. Near the transition, $T(t)$ falls off much slower (see figure 3) which yields to a much steeper dependence of $C(\Delta\omega)$ on $\Delta\omega$. The steeper dependence of $C(\Delta\omega)$ as we approach the transition is consistent with the results of Pendry and co-workers [49–50] who find an extremely steep fall-off for $C(\Delta\omega)$ for strongly localized states.

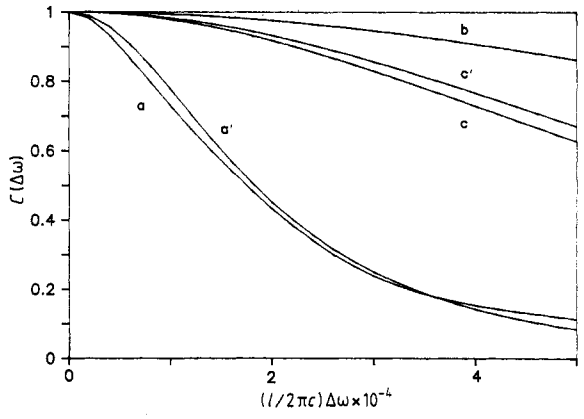

Figure 6. $C(\Delta\omega)$ for the transmitted wave as a function of $\Delta\omega$ for $L = 20\,l$. $\xi = 10\,l$. Curve a corresponds to $C(\Delta\omega)$ calculated for an anomalous pulse shape, curve a' for a normal pulse shape with a scale dependent diffusion constant. Curve b corresponds to $C(\Delta\omega)$ for a normal pulse shape. For an absorbing slab where the absorption length $L_a = 10\,l$, curve c corresponds to the anomalous pulse shape and curve c' to a normal pulse shape with a scale dependent diffusion constant.

We now include the effect of absorption by taking $L_a = 10l$. For this case, $C(\Delta\omega)$ as a function of $\Delta\omega/\omega$ is plotted in figure 6 (curve c). We see that $C(\Delta\omega)$ falls off much more slowly. This follows from the fact that the absorption cut-off Feynman path is longer than L_a. This leads to a much steeper fall-off of $T_{abs}(t)$ and a slower fall-off for $C(\Delta\omega)$ since t is a Fourier transform of $T_{abs}(t)$.

We now compare our results with an approximate approach in which we calculate $C(\Delta\omega)$ by using the normal pulse shape $T(t)$ (as given in the weak-disorder limit) but with a scale-dependent diffusion constant

$$D = D_0(L^{-1} + L_a^{-1} + \xi^{-1}) \tag{34}$$

Such an approach was used [22] recently to analyse the experiments near the optical Anderson transition. Curve a' in figure 6 represents the case $L = 20\,l$, $\xi = 10\,l$ and $L_a = \infty$. We see that this approach overestimates $C(\Delta\omega)$ for $\Delta\omega < \Delta\omega_{HW}$. This follows from the fact that the correct $T(t)$ falls off more slowly for large times. When absorption is included we expect similar behaviour. For $L_a = 10\,l$, we plot $C(\Delta\omega)$ as calculated from (33) (curve c').

We now turn to calculate $C(\Delta\omega)$ for reflected light. For $\Delta\omega < \Delta\omega_c$, we may write

$$C(\Delta\omega) = \left| \int e^{i\Delta\omega t} R(t)\, dt \right|^2 \tag{35}$$

where $R(t)$ is the pulse shape of the reflected light at a given point. Since $R(t)$ falls off much more steeply than $T(t)$, it follows that $C(\Delta\omega)$ for reflection decreases much more slowly than for transmission. The effect of the transition is to broaden $R(t)$ further, yielding a steeper decrease of $C(\Delta\omega)$. It should be noted that $T(t)$ and $R(t)$ refer to a *given* point at both boundaries and are not related. In figure 7(a), we plot $C(\Delta\omega)$ as a function of $\Delta\omega/\omega$ for anomalous diffusion (for which $R(t)$ is calculated by $D(t)$ as given by (7)). Figure 7(b) represents normal diffusion (for which $R(t)$ is calculated with $D = D_0 = 1/3Cl$). We see that the effect of the transition is to sharpen the decay of $C(\Delta\omega)$.

5. The dynamic autocorrelation function $C(\Delta t)$

Another property which generated much interest [35–40] in the weak disorder limit is the dynamic autocorrelation function $C(\Delta t)$ for dynamic disorder. $C(\Delta t)$ is defined as

$$C(\Delta t) = \langle I(t + \Delta t)I(t)\rangle - \langle I(t)\rangle^2)/\langle I(t)\rangle^2 \tag{36}$$

for a given change in time Δt. In the weak-disorder limit, two types of dynamic disorder

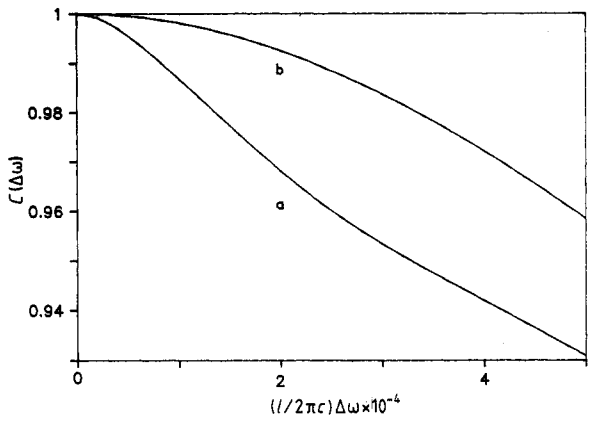

Figure 7. $C(\Delta\omega)$ for the reflected wave as a function of $\Delta\omega$ for $L = 20\,l$, $\xi = 10\,l$. Curve a corresponds to an anomalous pulse shape while curve b corresponds to a normal pulse shape.

were studied. In the first, the scatterers diffuse in time and each scatterer performs a random walk with a displacement δr given by $\langle \delta r^2(\Delta t)\rangle \propto \Delta t$. The second type of dynamic disorder corresponds to the case where each scatterer obeys a Maxwell–Boltzmann type of statistics. This means that each scatterer moves ballistically with a velocity $V = (2k_B T/M)^{1/2}$ (where T is the absolute temperature, k_B the Boltzmann constant and M the mass of the particle). For this type of disorder, the normalised autocorrelation function can also be related [35–40] to the random walk probability W_N for executing a Feynman trajectory of N steps. In the continuous approximation, $W_N \rightarrow T(t)$ where $T(t)$ is the pulse shape of the transmitted waves. In the factorisation approximation, we may write $C(\Delta t)$ as

$$C(\Delta t) = \left| \int \mathrm{d}t\, T(t) \exp\{-[r_{\mathrm{RMS}}^2(\Delta t)/\lambda^2]t/t_0\} \right|^2 \tag{37}$$

where $t_0 = l/2\pi^2 C$ and $r_{\mathrm{RMS}}^2(\Delta t) = \langle(\delta r(\Delta t))^2\rangle$.

The behaviour of $C(\Delta t)$ depends on the pulse shape $T(t)$ and the nature of the dynamic disorder due to $\delta r(\Delta t)$. Near the Anderson transition, $T(t)$ is given by (13) in the absence of absorption or by (15) in the presence of absorption. We can map the scaling behaviour of $C(\Delta t)$ on the scaling behaviour of $C(\Delta\lambda)$. We have already pointed out that $C(\Delta\omega)$ scales basically as $C(\Delta\omega t)$ where t is the average time needed to execute a trajectory of length Ct. The scaling behaviour of $C(\Delta t)$ can be deduced from $C(\Delta\omega)$ by replacing $\Delta\omega$ by $r_{\mathrm{RMS}}^2(\Delta t)$. Thus $C(r_{\mathrm{RMS}}^2(\Delta)t)$ will scale as $C(\Delta\omega t)$. We now take, for example, two types of dynamic disorder. For diffusive scatterers, $r_{\mathrm{RMS}}^2 \propto \Delta t$, and the scaling of $C(\Delta\omega t)$ is identical to $C(\Delta t \cdot t)$. Thus, the scaling behaviour of $C(\Delta t)$ for the first case studied (see table 1) may be obtained from $C(\Delta\omega)$ by simply replacing $\Delta\omega$ by Δt. For the second type of dynamic disorder, $r_{\mathrm{RMS}}^2 \propto (\Delta t)^2$. In this case, the scaling behaviour of $C(\Delta t)$ can be obtained from $C(\Delta\omega)$ by replacing $\Delta\omega$ in each equation by $(\Delta t)^2$. The six types of scaling behaviour of $C(\Delta t)$ for different regimes of Δt are given in table 2. It should be noted, however, that it would be much easier to measure $C(\Delta\lambda)$ than $C(\Delta t)$ near the transition. Indeed, initial measurements of $C(\Delta\lambda)$ near the transition were recently reported [22]. Due to strong absorption in their samples, the scaling behaviour as given in table 1 was not accessible.

Finally, $C(\Delta t)$ for reflected waves can be obtained by replacing $T(t)$ by $R(t)$ in (37).

Table 2. (*a*) $\langle \delta r^2(\Delta t) \rangle \propto \Delta t$, diffusive scatterers, where $\tau_\lambda = \lambda^2/4\pi^2 D_i$, D_i is the diffusion constant of the scatterers, (*b*) $\langle \delta r^2(\Delta t) \rangle \propto \Delta t^2$, ballistic scatterers, where $t_\lambda = (m\beta\lambda^2/2\pi^2)^{1/2}$, $\beta = 1/K_B T$.

	$\Delta t < \frac{2}{3}(l/\xi)^3 \tau_i$	$\Delta t > \frac{2}{3}(l/\xi)^3 \tau_i$
$L < \xi$	$C(\Delta t L^3)$	
$L > \xi$	$C(\Delta t L^2 \xi)$	$C(\Delta t^{1/3} L)$
	$\Delta t^2 < \frac{2}{3}(l/\xi)^3 \tau^{2zs}_\lambda$	$\Delta t^2 > \frac{2}{3}(l/\xi)^3 \tau$
$L < \xi$	$C(\Delta t^2 L^3)$	
$L > \xi$	$C(\Delta t^2 L^2 \xi)$	$C(\Delta t^{2/3} L)$

6. The memory effect

The memory effect, which was recently predicted by Feng *et al* [29] and observed experimentally by Freund *et al* [42] connects the sensitivity of the scattered waves to a change in the direction of the incident wave vector $\Delta \boldsymbol{q}_i = \boldsymbol{q}_i' - \boldsymbol{q}_i$. The autocorrelation function $C(\Delta \boldsymbol{q}_i, \Delta \boldsymbol{q}_f) = \langle I(\boldsymbol{q}_i, \boldsymbol{q}_f), I(\boldsymbol{q}_i', \boldsymbol{q}_f') \rangle$ (where $\Delta \boldsymbol{q}_f = \boldsymbol{q}_f' - \boldsymbol{q}_f'$ is the change in direction of the transmitted wave and similarly for $\Delta \boldsymbol{q}_i$) was recently calculated in real space by Berkovits *et al* [43]. The only relevant quantity that enters $C(\Delta \boldsymbol{q}_i, \Delta \boldsymbol{q}_f)$ is the diffusive probability for a given trajectory that started at position $\boldsymbol{R}_1$ on the incoming boundary to arrive at point $\boldsymbol{R}_2$ at the outgoing boundary. Since the diffusive range $|\boldsymbol{R}_2 - \boldsymbol{R}_1|$ for transmitted waves must be of order L, $C(\Delta \boldsymbol{q}_i, \Delta \boldsymbol{q}_f)$ must scale as $\Delta q_i L$ with $\Delta q_i = \Delta q_f$ and to fall-off substantially for $\Delta q_i L < 1$. Near the Anderson transition when anomalous diffusion sets in, the range $|\boldsymbol{R}_2 - \boldsymbol{R}_1|$ is expected to be smaller since longer trajectories are less probable. We therefore expect the memory correlation function to be broader. On the other hand, since the diffusion constant does not enter the expression $C(\Delta \boldsymbol{q}_i, \Delta \boldsymbol{q}_f)$ for transmitted waves in the weak disorder limit, we expect only a small change in its shape when the transition is reached. Our expression for the memory correlation function near the transition is

$$C(\Delta \boldsymbol{q}_i, \Delta \boldsymbol{q}_f) = \delta_{\Delta \boldsymbol{q}_i, \Delta \boldsymbol{q}_f} \left(\int \mathrm{d}t \, T(t) \exp(-\tfrac{3}{2} D_0 \tau^{1/3} \Delta q_i^2 t^{2/3}) \right)^2 \tag{38}$$

If figure 8, we plot $C(\Delta \boldsymbol{q}_f)$ as a function of Δq_f near the transition. We see that the memory correlation function is somewhat broader (dashed curve) than for normal diffusion (solid curve) but essentially not affected by the transition. The correlation function should be relevant only for a heterodyne experiment where electric field correlation functions are measured directly. For intensity–intensity correlation functions, $C(\Delta \boldsymbol{q}_i, \Delta \boldsymbol{q}_f)$ must include all higher-order corrections which may substantially modify the result. These corrections cannot be handled within the scaling approach we use here.

We now turn to the memory effect for backscattered waves. Here the diffusive range $|\boldsymbol{R}_i - \boldsymbol{R}_2|$ must be a few mean free paths. Indeed, the explicit expression for $C(\Delta \boldsymbol{q}_i, \Delta \boldsymbol{q}_f)$ in the weak disorder limit depends on the diffusion constant. Near the Anderson transition, $D \to 0$ and the range is smaller. This must lead to an *improved* memory effect. Namely, as $\xi \to \infty$, $C(\Delta q_f)$ falls off much slower as a function of Δq_f. This is demonstrated in figure 9. We see that the memory effect for backscattered waves behaves in a similar

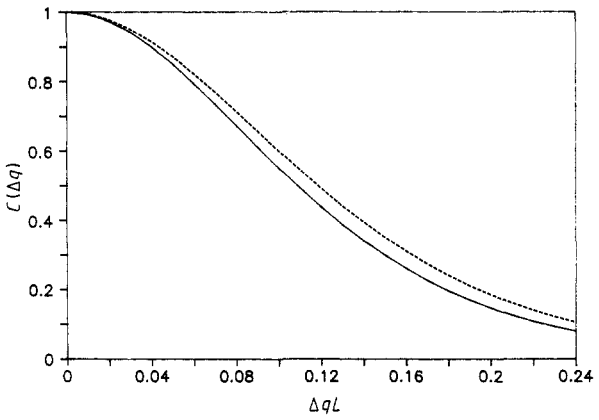

Figure 8. The memory correlation function $C(\Delta q)$ as a function of Δq for the transmitted wave. The full curve is for a normal pulse shape, while the broken curve is for the pulse shape when $\xi = 10^4 l$. The slab width $L = 20 l$.

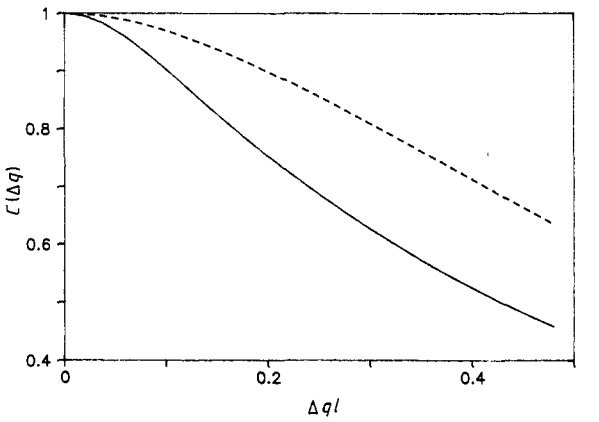

Figure 9. The memory correlation function $C(\Delta q)$ as a function of Δq for the reflected wave. The full curve is for a normal pulse shape, while the broken curve is for the pulse shape when $\xi = 10^4 l$. The slab width $L = 20 l$.

manner to the coherent backscattered peak which becomes broader near the transition [45]. Indeed, it was recently pointed out [53] that the correlation function $C(\Delta q_f)$ is intimately related to the form of the enhanced coherent background peak.

7. Summary

We have used a local scaling approach to calculate the ensemble averaged pulse shape function $T(t)$ for waves transmitted through a slab. We have shown that the total transmission coefficient T as deduced from our $T(t)$ is consistent with the global scaling approach introduced by Anderson[2]. We then relate the intensity–intensity autocorrelation function $C(\Delta\lambda)$ to the pulse shape $T(t)$. It is shown that three different scaling forms emerge which we have summarised in table 1.

We have also calculated the dynamic autocorrelation function $C(\Delta t)$ near the Anderson transition. The scaling behaviour of $C(\Delta t)$ is also related to the functional form of the transmitted pulse shape $T(t)$. We have given a simple mapping between $C(\Delta t)$ and $C(\Delta\lambda)$ in which the scaling behaviour of $C(\Delta t)$ can be obtained from the scaling behaviour

of $C(\Delta\lambda)$. This is summarised in table 2. We have also studied $C(\Delta t)$ and $C(\Delta\lambda)$ for reflected waves near the transition.

Finally, we have studied the effect of the Anderson transition on the memory effect. it is shown that the transition broadens the memory correlation function. Although this effect is quite small for transmitted waves, it is dramatic for backscattered waves.

Acknowledgments

We are grateful to the Israeli–US Binational Science Foundation and The Israeli Academy of Science and Humanities for supporting this work.

References

[1] John S 1984 *Phys. Rev. Lett.* **53** 2169; 1985 *Phys. Rev.* B **31** 304
[2] Anderson P W 1985 *Phil. Mag.* B **52** 505
[3] Ioffe A F and Regel A R 1960 *Prog. Semicond.* **4** 237
[4] Mott N F and Davis E A 1979 *Electronic Processes in Non-Crystalline Materials* (Oxford: Oxford University Press)
[5] Lee P A and Raakrishnan T V 1985 *Rev. Mod. Phys.* **57** 287
[6] Mott N F and Kaveh M 1985 *Adv. Phys.* **34** 329
[7] Fritzche H and Adler D (ed) 1985 *Localization and Metal–Insulator Transitions* (New York: Plenum)
[8] Thomas G 1984 *Phil. Mag.* B **50** 169 and references therein
[9] Kaveh M 1987 *Disordered Semiconductors* M A Kastner, G A Thomas and S R Ovshinsky (ed) (New York: Plenum)
[10] Kaveh M 1985 *Phil. Mag. Lett.* B **52** L1
[11] Castellani C, Kotliar G and Lee P A 1987 *Phys. Rev. Lett.* **59** 923
[12] Kaveh M and Mott N F 1987 *Phil. Mag.* B **55** 1; 1987 *Phil. Mag.* B **55** 9
[13] Cohen S M and Machta J 1985 *Phys. Rev. Lett.* **54** 2242
Cohen S M, Machta J, Kirkpatrick T R and Condat C A 1987 *Phys. Rev. Lett.* **58** 785
[14] Arya K, Su Z B and Birman J L 1986 *Phys. Rev. Lett.* **57** 2725
[15] Sheng P and Zhang Z Q 1986 *Phys. Rev. Lett.* **57** 1879
[16] John S 1987 *Phys. Rev. Lett.* **58** 2486
[17] Kaveh M 1987 *Phil. Mag.* B **56** 693
[18] Soukolis C M, Economou E N, Grest G S and Cohen M 1989 *Phys. Rev. Lett.* **62** 575
Economou E N and Soukoulis C M 1989 *Phys. Rev.* B **40** 7977
[19] Abrahams E, Anderson P W, Licciardello D C and Ramakrishnan T V 1979 *Phys. Rev. Lett.* **42** 673
[20] Altshuler B L, Kravtsov V E and Lerner I 1986 *JETP Lett.* **43** 441
Efetov K B 1984 *JETP Lett.* **40** 738
Kumar N and Jayanavar A M 1986 *J. Phys. C: Solid State Phys.* **191** L85
[21] Shapiro B 1985 *Phys. Rev.* B **34** 4396; 1987 *Phil. Mag.* **56** 1031
Cohen A, Roth Y and Shapiro B 1989 *Phys. Rev.* B **38** 12125
[22] Genack A Z 1989 *Classical Waves Localization* ed P Sheng (Singapore: World Scientific)
Genack A Z and Drake J M 1989 *Phys. Rev. Lett.* **63** 259
[23] Imry Y 1980 *Phys. Rev. Lett.* **44** 469
[24] Genack A Z 1987 *Phys. Rev. Lett.* **58** 2059
[25] Shapiro B 1986 *Phys. Rev. Lett.* **57** 2168
[26] Stephen M J and Cwilich 1975 *Phys. Rev. Lett.* **59** 285
Pnini R and Shapiro B 1989 *Phys. Rev.* B **39** 6986
[27] Edrei I and Kaveh M 1988 *Phys. Rev.* B **38** 950
[28] Edrei I and Kaveh M 1989 *Phys. Rev.* B **40** 9419
[29] Feng S, Kane C, Lee P A and Stone A D 1988 *Phys. Rev. Lett.* **61** 834
[30] For the first observations of enhanced coherent backscattering, see
Kuga Y and Ishimaru I 1984 *J. Opt. Soc. Am.* A **1** 831
Van Albada M P and Lagendijk A 1985 *Phys. Rev. Lett.* **55** 2692

Wolf P E and Maret G 1985 *Phys. Rev. Lett.* **55** 2696
Etemad S, Thompson R and Andrejco M J 1986 *Phys. Rev. Lett.* **57** 575
Kaveh M, Rosenbluh N, Edrei I and Freund I 1986 *Phys. Rev. Lett.* **51** 2049
[31] Akkermans E A, Wolf P E and Maynard R 1986 *Phys. Rev. Lett.* **56** 1471
Edrei I and Kaveh M 1987 *Phys. Rev.* B **35** 6761
Van Albada M P and Lagendijk A 1987 *Phys. Rev.* B **36** 2353
[32] Van Albada M P, Van der Mark M B and Lagendijk A 1987 *Phys. Rev. Lett.* **57** 2049
Akkermans E, Wolf P E, Maynard R and Maret G 1988 *J. Physique* **49** 77
[33] For the role of different Feynman path on the shape of the coherent backscattering, see
Rosenbluh M, Freund I, Edrei I and Kaveh M 1987 *Phys. Rev.* A **35** 4458
Etemad S, Thompson R, Andrejco M J, John S and Mackintosh F 1987 *Phys. Rev. Lett.* **59** 1420
Van der Mark M B, Van Albada M P and Lagendijk A 1988 *Phys. Rev.* B **37** 3575
Wolf P E, Akkermans E and Maynard R 1988 *J. Physique* **49** 63
[34] For coherent backscattering in two-dimensional systems see
Freund I, Rosenbluh M, Berkovits R and Kaveh M 1988 *Phys. Rev. Lett.* **61** 1214
Berkovits R and Kaveh M 1987 *J. Phys. C: Solid State Phys.* **20** L181
[35] Kaveh M, Rosenbluh M and Freund I 1987 *Nature (London)* **326** 778
Rosenbluh M, Freund I, Hoshen M and Kaveh M 1987 *Phys. Rev. Lett.* **58** 2754
[36] Maret G and Wolf P E 1987 *Z. Phys.* B **65** 109
[37] Freund I, Kaveh M and Rosenbluh M 1988 *Phys. Rev. Lett.* **60** 1130
[38] Pine D J, Weitz D A, Chaikin P M and Herbalzheimer E 1988 *Phys. Rev. Lett.* **60** 1134
[39] Stephen M J 1988 *Phys. Rev.* B **37** 1
[40] Edrei I and Kaveh M 1988 *J. Phys. C: Solid State Phys.* **21** L971
[41] Watson G H Jr, Fleury P A and McCall S L 1987 *Phys. Rev. Lett.* **59** 945
[42] Freund I, Rosenbluh M and Feng S 1988 *Phys. Rev. Lett.* **61** 2328
[43] Berkovits R, Kaveh M and Feng S 1989 *Phys. Rev.* B **40** 737
[44] Imry Y and Gefen Y 1984 *Phil. Mag.* B **50** 203
Abrahams E and Lee P A 1986 *Phys. Rev. Lett.* **33** 683
[45] Berkovits R and Kaveh M 1987 *Phys. Rev.* B **36** 9322
[46] Berkovits R, Edrei I and Kaveh M 1989 *Phys. Rev.* B **39** 12250
[47] Morse P M and Feshbach H 1953 *Methods of Theoretical Physics* (New York: McGraw-Hill)
[48] For values of Δ for lower dimensions, see [34]
[49] Pendry J P and Kirkman P 1984 *J. Phys. C: Solid State Phys.* **17** 6711–6722
[50] Kirkman P and Pendry J B 1986 *J. Phys. C: Solid State Phys.* **19** 207–220
[51] Pendry J B 1987 *J. Phys. C: Solid State Phys.* **20** 733–742
[52] Pendry J B 1988 *J. Res. Dev.* **32** 137–143
[53] Freund I, Rosenbluh M and Berkovits R 1989 *Phys. Rev.* B **39** 12403